Extremophiles (2011) 15:337–346
DOI 10.1007/s00792-011-0365-4

ORIGINAL PAPER

Biochemical characterization of glyceraldehyde-3-phosphate dehydrogenase from *Thermococcus kodakarensis* KOD1

Baolei Jia · Le Thuy Linh · Sangmin Lee · Bang Phuong Pham · Jinliang Liu · Hongyu Pan · Shihong Zhang · Gang-Won Cheong

Received: 1 November 2010 / Accepted: 28 February 2011 / Published online: 16 March 2011

Abstract Glyceraldehyde-3-phosphate dehydrogenase (GAPDH) plays an essential role in glycolysis by catalyzing the conversion of D-glyceraldehyde 3-phosphate (D-G3P) to 1,3-diphosphoglycerate using NAD^+ as a cofactor. In this report, the GAPDH gene from the hyperthermophilic archaeon *Thermococcus kodakarensis* KOD1 (GAPDH-tk) was cloned and the protein was purified to homogeneity. GAPDH-tk exists as a homotetramer with a native molecular mass of 145 kDa; the subunit molecular mass was 37 kDa. GAPDH-tk is a thermostable protein with a half-life of 5 h at 80–90°C. The apparent K_m values for NAD^+ and D-G3P were 77.8 ± 7.5 μM and 49.3 ± 3.0 μM, respectively, with V_{max} values of 45.1 ± 0.8 U/mg and 59.6 ± 1.3 U/mg, respectively. Transmission electron microscopy (TEM) and image processing confirmed that GAPDH-tk has a tetrameric structure. Interestingly, GAPDH-tk migrates as high molecular mass forms (~232 kDa and ~669 kDa) in response to oxidative stress.

Keywords GAPDH · Thermophilic protein · Oxidative stress · Protein aggregation · TEM

Communicated by T. Matsunaga.

B. Jia and L. T. Linh contributed equally.

Electronic supplementary material The online version of this article (doi:10.1007/s00792-011-0365-4) contains supplementary material, which is available to authorized users.

B. Jia · J. Liu · H. Pan · S. Zhang
College of Plant Sciences, Jilin University, Changchun 130-062, China

B. Jia · L. T. Linh · S. Lee · B. P. Pham · G.-W. Cheong (✉)
Division of Applied Life Sciences (BK21 Program), Gyeongsang National University, Jinju 660-701, Korea
e-mail: gwcheong@gnu.ac.kr

G.-W. Cheong
Environmental Biotechnology National Core Research Center, Gyeongsang National University, Jinju 660-701, Korea

Introduction

Glyceraldehyde-3-phosphate dehydrogenase (GAPDH) is an enzyme in the glycolytic pathway that catalyzes the phosphorylation of glyceraldehyde-3-phosphate to form 1,3-bisphosphoglycerate. The reaction catalyzed by GAPDH is the sum of two processes: the oxidation of the aldehyde to a carboxylic acid by NAD^+ and the joining of the carboxylic acid and an orthophosphate to form the acyl-phosphate product. This enzyme occurs universally throughout the bacterial, eukaryotic, and archaeal domains of life (Brunner et al. 1998).

GAPDH has been studied in many organisms, including archaea. The archaeal enzymes share less identity with bacterial and eukaryotic GAPDH (16–20%) and display dual cofactor specificity for NAD^+ and $NADP^+$ (Littlechild and Isupov 2001), in contrast to the bacterial and eukaryotic enzymes, which are usually specific for NAD^+ (Brunner et al. 1998, 2001). The GAPDH from *Methanothermus fervidus* reacts with both NAD^+ and $NADP^+$ and is not inhibited by pentalenolactone (Stefan et al. 1988). *Sulfolobus solfataricus* GAPDH is able to use both NAD^+ and $NADP^+$, but exhibits a marked preference for $NADP^+$ (Carol et al. 1995). In addition, many archaea, including *Thermoproteus tenax*, also harbor a structurally distinct non-phosphorylating glyceraldehyde-3-phosphate dehydrogenase, referred to as GAPN (Lorentzen et al. 2004).

However, recent evidence demonstrates that GAPDH is a multifunctional protein (Tristan et al. 2010). Roles for GAPDH in membrane transport and membrane fusion (Tisdale 2001), microtubule assembly (Launay et al. 1989), phosphotransferase activities (Engel et al. 1998), nuclear RNA export, DNA replication, and DNA repair (Sirover 1996) have been documented. In addition to the various functions of GAPDH described above, GAPDH is frequently associated with oxidative stress. Nitric oxide (NO) is one of the major cellular signaling molecules and is known to mediate cell death. GAPDH has received particular attention as a major target of NO in cells, following the discovery of NO-induced ADP ribosylation of GAPDH, which inhibits its glycolytic activity (Hara et al. 2005; Hara and Snyder 2006).

Although GAPDH has previously been examined in thermophilic archaea, the non-glycolytic properties of archaeal GAPDH have not been investigated. In this report, we cloned and overexpressed GAPDH from *Thermococcus kodakarensis* KOD1 (GAPDH-tk) (Atomi et al. 2004). We have biochemically characterized the enzyme and used mutants to analyze the catalytic mechanism. The quaternary structure of GAPDH was observed by TEM and image processing. Lastly, we tested the effect of oxidative stress on the native conformation of the protein.

Materials and methods

Cloning of GAPDH-tk from *T. kodakarensis* KOD1

Polymerase chain reaction (PCR) with *T. kodakarensis* KOD1 genomic DNA as a template was performed to isolate GAPDH-tk using the oligonucleotide primers: forward, 5′-GGA ATT CCA TAT GAA GGT GAA AGT C-3′; and reverse, 5′-CCG CTC GAG TCA CTT CAG AAT TCC AA-3′). The PCR products were ligated into the pET28(a) vector, transformed into *Escherichia coli* BL21 (DE3), and sequenced.

Expression and purification of GAPDH-tk

E. coli BL21(DE3) cells containing the pET28a-GAPDH-tk plasmid were cultured in 2 l of LB broth with 30 μg/ml kanamycin at 37°C for 3 h. When the OD_{600} reached 0.7, isopropyl-β-D-thiogalactopyranoside (IPTG) was added to induce protein expression. The cells were cultured in the presence of IPTG for 4 h with shaking, harvested by centrifugation at 6,000 rpm for 10 min, and then resuspended in lysis buffer containing 50 mM Tris (pH 8.0), 300 mM NaCl, 20 mM 2-mercaptoethanol, and 20 mM imidazole. The cell suspension was sonicated and heated at 65°C for 1 h. The thermostable components in the supernatant were collected following centrifugation and loaded on an Ni–NTA column. After washing the column with lysis buffer, GAPDH-tk was eluted using an imidazole gradient (50–250 mM). The purified GAPDH-tk was visualized after separation by 12.5% sodium dodecyl sulfate polyacrylamide gel electrophoresis (SDS-PAGE). The eluted proteins were dialyzed against 50 mM Tris buffer (pH 8.0) containing 300 mM NaCl and 20 mM 2-mercaptoethanol. Protein concentrations were estimated by the method of Bradford using bovine serum albumin (BSA) as a standard.

Gel filtration chromatography

Gel filtration chromatography was performed using a Superdex 200 10/30 column (GE Healthcare) on an FPLC system (BIO-RAD). The column was equilibrated with 50 mM Tris, 300 mM NaCl, and 20 mM 2-mercaptoethanol, pH 8.0. Protein standards included thyroglobulin (669 kDa), ferritin (440 kDa), catalase (232 kDa), aldolase (158 kDa), albumin (67 kDa), and ovalbumin (43 kDa). Collected protein samples were examined by SDS-PAGE and native PAGE.

Site-directed mutagenesis of GAPDH-tk

The primers used for the single cysteine to serine mutant were as follows: forward, 5′-GTC GTC TCC AGT AAC ACG ACT -3′; reverse, 5′-AGT CGT GTT ACT GGA GAC GAC-3′. The pET28a-GAPDH-tk plasmid was used as the DNA template. The PCR reaction was performed for 18 cycles (94°C for 30 s, 55°C for 1 min and 68°C for 12 min). After amplification, the PCR mixture was digested with *Dpn*I and used to transform *E. coli* BL21(DE3). The mutant was confirmed by DNA sequencing. The GAPDH-C141S protein was purified by the same methods as that of the wild-type protein, as described above.

Enzyme assays

GAPDH enzyme activity was measured by following the increase in absorbance at 340 nm at 80°C when the enzyme was incubated in a standard assay mixture (total volume 1.0 ml) that contained 50 mM Tris/HCl (pH 7.0), 20 mM 2-mercaptoethanol, 10 mM potassium arsenate, 10 mM D-glyceraldehyde-3-phosphate (D-G3P), and 1 mM NAD^+. To analyze the effect of phosphate, 10 mM potassium phosphate was added in the reaction system if necessary. Glyceraldehyde-3-phosphate is thermolabile and was therefore added immediately before the reaction was started by the addition of the enzyme. Unlike D-G3P, NAD^+ is stable up to 70°C (Stefan et al. 1988).

The enzyme activity was determined from the initial velocity of the reaction. One unit GAPDH-tk activity is

defined as the amount of enzyme that catalyzes the formation of 1 μmol NADH/min under the conditions of the assay. The specific activity of the enzyme is determined by the ratio of enzyme activity to the amount of protein in the assay.

Although NADH is not stable at higher temperatures and therefore the measurement of NADH-producing enzymatic reactions will tend to underestimate the enzyme activities, there is only a 0.4% difference between the directly measured increase in absorption and the increase in absorption corrected for NADH decay up to 70°C (Stefan et al. 1988).

Kinetic study

For kinetic studies, the initial velocities of the enzymatic reaction were examined by varying the concentration of D-G3P (from 0.04 to 10 mM), phosphate (from 0.04 to 10 mM) or NAD^+ (from 0.02 to 2 mM). Values of the Michaelis constants (K_m), dissociation constants (k_{cat}), and maximal velocity (V_{max}) were obtained by mathematical calculations according to the method of Cleland (1963).

Effect of oxidative stress on GAPDH-tk

GAPDH-tk was treated with 1 mM H_2O_2 or 1 mM sodium nitroprusside (SNP), a NO donor. The mixtures were incubated at 80°C for 1 h. After treatment, the proteins were analyzed by gel filtration chromatography, native PAGE, and TEM.

Electron microscopy and image processing

Samples of purified GAPDH-tk in a buffer containing 50 mM Tris (pH 8.0), 300 mM NaCl, and 20 mM 2-mercaptoethanol were placed on glow-discharged carbon-coated copper grids. After allowing the protein to adsorb for 1–2 min, the grids were rinsed with deionized water and stained with 2% (w/v) uranyl acetate. Specimens were examined in an FEI Technai-12 transmission electron microscope at an acceleration voltage of 120 kV using a low-dose unit (Park et al. 2006). Electron micrographs were recorded on Kodak film (SO163) at a nominal magnification of ×67,000. Light-optical diffractograms were used to select the micrographs, to examine the defocus, and to verify that no drift or astigmatism was present. Suitable areas were digitized as arrays of 1,024 × 1,024 pixels using Leaf Scan 45 at a pixel size of 20 μm corresponding to 0.30 nm at the specimen level. For image processing, the SEMPER (Saxton et al. 1979) and EM (Hegerl 1996) software packages were used. From digitized micrographs, smaller frames of 32 × 32 pixels containing individual particles were extracted. These images were aligned translationally and rotationally using standard correlation methods (Kim et al. 2000). For analyzing the rotational symmetry of top-on view images, the aligned images were subjected to multivariate statistical analysis (Van Heel and Frank 1981). The individual images were aligned translationally but not rotationally as described by Marco et al. (1994). The resulting eigenimages represent all the important structural features of the original data set. If the images have different rotational symmetries in the original data set, the eigenimages reveal the different symmetry axes. Moreover, these images can be distinguished and, subsequently, separated based on eigenimages. The rotationally aligned images were classified based on eigenvector–eigenvalue data analysis, and subsequent averaging was performed for each class separately.

Results

Alignment of the GAPDH-tk sequence with homologous sequences

The DNA sequence encoding GAPDH-tk (Tk0765) has an open reading frame of 1,005 nucleotides, indicating that GAPDH-tk is composed of 334 amino acids with a predicted molecular mass of ~37 kDa. GAPDH homologs were found using BLAST in the NCBI database. Sequences were aligned using Clustal W. GAPDH-tk exhibited high identity to previously characterized GAPDH from archaea, such as the GAPDH from *S. solfataricus* (Sso0528) (46%) (Littlechild and Isupov 2001) and *M. fervidus* (Mfe0276) (54%) (Stefan et al. 1988), but much lower identity to GAPDH from *Bacillus stearothermophilus* (16%) (Roitel et al. 1999), *E. coli* (16%) (Z2818) (Yun et al. 2000), *Homo sapiens* (CDABP0047) (human, 13%) (Elkina et al. 2010), and *Rattus norvegicus* (rat, 13%) (Fig. 1). GAPDH-tk and homologs share one conserved N-terminal domain: a Rossmann-fold NAD(P)H/NAD(P)(+) binding (NADB) domain. The NADB domain is found in many dehydrogenases from metabolic pathways such as glycolysis, as well as many other redox enzymes. GAPDH-tk contains the characteristic GYGTIG sequence, a consensus binding sequence in which the first two glycines participate in NAD(P)-binding and the third facilitates close packing of the helix to the adjacent beta-strand of the protein. In contrast to GAPDH from *S. solfataricus*, which has three cysteine residues, one in the nucleotide-binding domain and two in the catalytic domain, GAPDH-tk has only one cysteine, C141, which is conserved in the same topological position as the active site C139 of the GAPDH from *S. solfataricus* (Isupov et al. 1999; Littlechild and Isupov 2001).

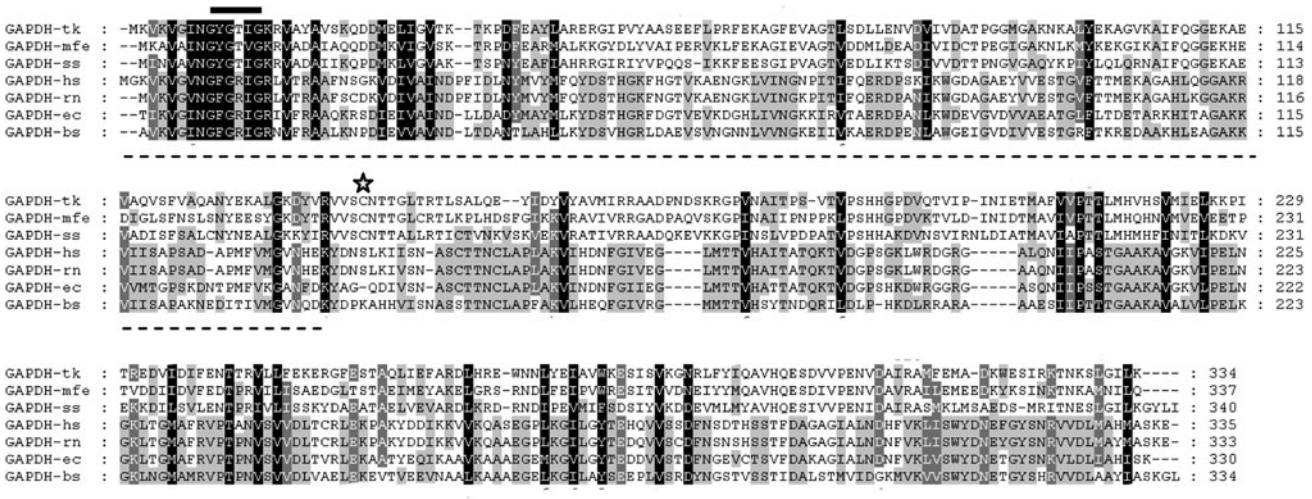

Fig. 1 Multiple amino acid alignment of GAPDH homologs. GAPDH sequences from *T. kodakarensis* KOD1 (GAPDH-tk, Q5JHB5), *M. fervidus* (GAPDH-mfe, 1CF2Q), *S. solfataricus* (GAPDH-ss, P39460), *Homo sapiens* (GAPDH-hs, P04406), *Rattus norvegicus* (GAPDH-rn, P04797), *E. coli* (GAPDH-ec, NP_288215), and *B. stearothermophilus* (GAPDH-bs, P00362) were aligned. The *broken line* indicates the Rossmann-fold NAD(P)H/NAD(P)$^+$ binding (NADB) domain. The consensus binding pattern GYGTIG conserved in the NADB domain is shown by the *solid line*. The *asterisk* shows the position of the cysteine residue

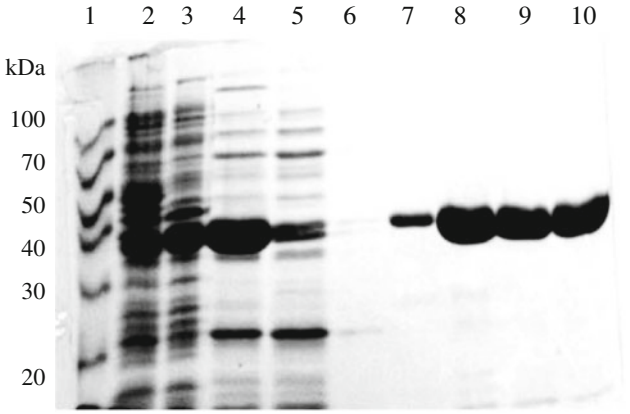

Fig. 2 Purification of GAPDH-tk. *Lane 1* protein markers; *lane 2* crude protein extract from non-induced cells; *lane 3* crude protein extract from IPTG-induced cells; *lane 4* soluble extract after heating at 65°C for 1 h; *lane 5* unbound proteins eluted from the Ni–NTA column; *lane 6*, proteins eluted by lysis buffer; *lane 7–10* proteins eluted by 50 mM imidazole, 100 mM imidazole, and 250 mM imidazole. The molecular mass standards are indicated on the *left*

Purification of GAPDH-tk

The gene encoding GAPDH-tk was cloned and overexpressed in *E. coli* (Fig. 2a). GAPDH-tk was purified by heating a total protein extract of the induced cells and removing the denatured proteins by centrifugation. The thermostable GAPDH-tk in the supernatant was then purified using an Ni–NTA column (Fig. 2). The molecular mass of purified GAPDH-tk was approximately 37 kDa, which is close to the molecular mass calculated from amino acids sequence. Unlike GAPDH from *M. fervidus* (∼45 kDa) (Charron et al. 2000), the molecular mass of subunits of GAPDH-tk is similar to the hyperthermophilic archaeon *S. solfataricus* (∼39 kDa) (Littlechild and Isupov 2001) and eukaryotic GAPDHs such as rabbit (∼36 kDa) (Nakajima et al. 2007) and the European pilchard *Sardina pilchardus* (∼37 kDa) (Baibai et al. 2007) based on SDS-PAGE gels and protein primary structure.

To examine the native structure of GAPDH-tk, the purified protein was analyzed by gel filtration chromatography and native PAGE (Fig. S1). One peak eluted from the gel filtration column at approximately 145 kDa. Purified GAPDH-tk fractions from this peak were analyzed by native PAGE and SDS-PAGE (Fig. S1). The native molecular mass of GAPDH-tk is ∼145 kDa. These results indicate that GAPDH-tk is a tetramer of 37 kDa subunits, which is similar to GAPDHs in both archaea and eukarya (Littlechild and Isupov 2001; Nakajima et al. 2007; Baibai et al. 2007).

Activity of GAPDH-tk

The influence of pH and temperature on purified GAPDH-tk activity was examined. The specific activity of purified GAPDH-tk was examined in the pH range 6.2–9.0 using a mixture of different buffers including sodium phosphate, HEPES, and Tris (Fig. 3A). The pH optimum for enzyme activity was approximately 7.0, which is well within the pH range (pH 5.0–9.0) suitable for the growth of *T. kodakarensis* KOD1. The GAPDH-tk pH optimum was substantially different from the GAPDH of the hyperthermophilic *M. fervidus* (optimal pH ∼8.5) (Stefan et al. 1988), which reflects the differences in environmental conditions of these organisms. GAPDH-tk activity was measured at

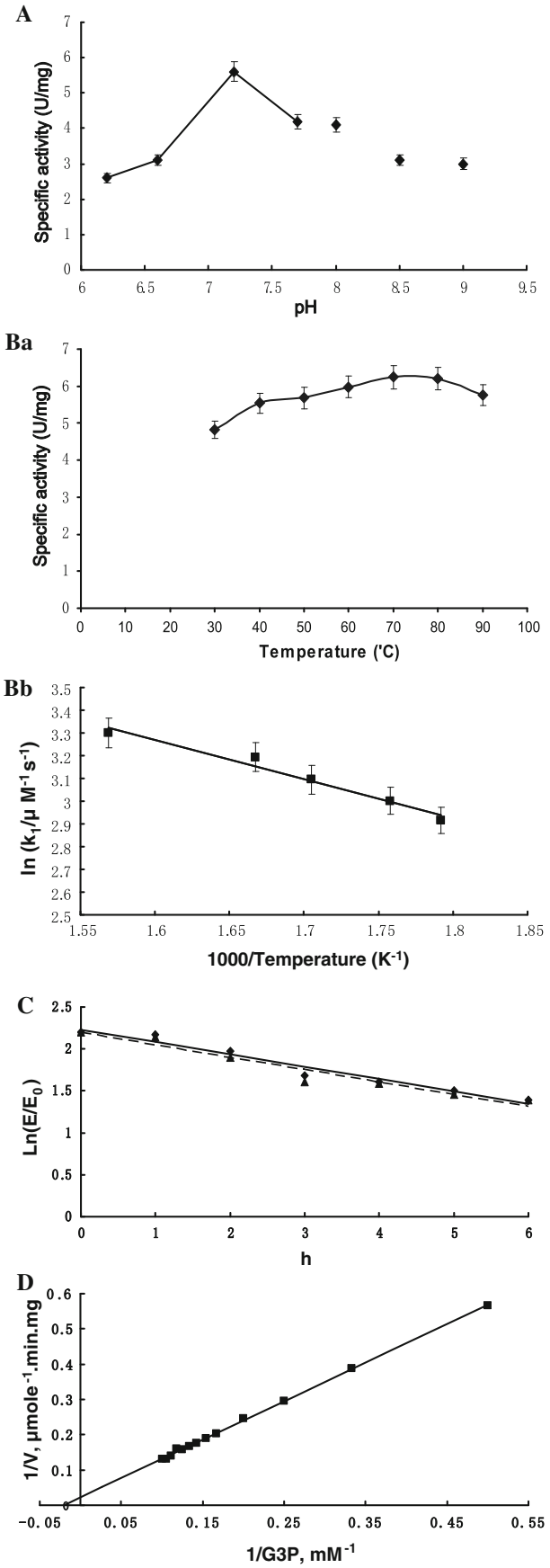

◀ **Fig. 3** Effects of pH and temperature on GAPDH-tk activity. **A** Optimal pH of GAPDH activity. Different buffers were used for the different pH solutions used in this assay. Sodium phosphate was used for pH 6.2, 6.6, 7.2, and 7.7; Hepes buffer and Tris buffer were used for pH 8.0 and 8.5; sodium borate buffer was used for pH 9.0. The concentrations of the buffers were 50 mM. **B** (**a**) Optimal temperature of GAPDH-tk activity. (**b**) Arrhenius plot for the reaction. *Solid line* is linear fit ($R^2 = 0.97$), with intercept of $\ln(A) = 6.03$, and slope of 1.73 corresponding to an Arrhenius activation energy of Ea = 13.84 kJ mol^{-1}. **C** Semi-logarithmic plots for the inactivation of GAPDH-k at 80°C (*filled diamonds*) and at 90°C (*filled triangles*). The trend lines at 80 and 90°C are shown by a *solid line* and *broken line*, respectively. Values are the means of three independent experiments. **D** Double reciprocal plots of initial velocity of GAPDH-tk at different D-G3P concentrations. The assays were carried out a as described under "Materials and methods"

temperatures from 30 to 90°C (Fig. 3Ba) and exhibited high activity from 70 to 90°C with activation energy of 13.84 kJ mol^{-1}, calculated using the corresponding linear Arrhenius plot (Fig. 3Bb). The activation energy of GAPDH-tk is lower than GAPDH of *Thermotoga maritima* (78.6–32.8 kJ mol^{-1}) (Wrba et al. 1990), *Synechococcus* sp. (20.6 kJ mol^{-1}) (Sand et al. 1994) and *S. sulfolobus* (55 kJ mol^{-1}) (Russo et al. 1995), but higher than GAPDH of dromedary camel (4.9 kJ mol^{-1}) (Fourrat et al. 2007).

The thermostability of GAPDH-tk was examined at 80 and 90°C (Fig. 3C). GAPDH-tk was incubated from 1 to 8 h at the indicated temperatures and enzyme activity was then tested. The results demonstrate that GAPDH-tk is thermostable with enzymatic activity half-life of 4.5 and 4.8 h at 80 and 90°C, respectively. GAPDH-tk has a shorter half-life of activity than the hyperthermophilic GAPDH of *S. solfataricus* at 80°C, which has a half-life of 17 h (Carol et al. 1995). The half-life of the *P. woesei* GAPDH is 65 min at 97°C (Zwickl et al. 1990). GAPDH-tk catalyzes a two-substrate reaction. The K_m values for NAD$^+$ and D-G3P were determined by varying the concentration of one substrate (D-G3P or NAD$^+$), while maintaining a constant concentration of the other substrate (Fig. 3D). The kinetic parameters reported here are the mean of three determinations ± SE. The K_m values for NAD$^+$ and D-G3P were 77.8 and 49.3 μM, respectively (Table 1). The V_{max} for NAD$^+$ and D-G3P were calculated to be 45.1 and 59.6 U/mg, respectively. To measure kinetic parameters for phosphate, 10 mM phosphate was added in the reaction system. The results showed that K_m and V_{max} for phosphate were 54.6 μM and 52.8 U/mg in the fixed concentration of D-G3P and NAD$^+$. A comparison of kinetic parameters of GAPDH-tk and GAPDH from other organisms is shown in Table 1.

The active site of GAPDH-tk

The active site of GAPDH contains a cysteine residue: C139 in *S. solfataricus* (Isupov et al. 1999), C150 in rat and C152 in humans (Hara and Snyder 2006). GAPDH-tk has

Table 1 Kinetic parameters for oxidation reaction of GAPDH-tk

Organisms	Kinetic parameters					
	K_m NAD^+ (μM)	V_{max} NAD^+ (U/mg)	K_m D-G3P (μM)	V_{max} D-G3P (U/mg)	K_m phosphate (μM)	V_{max} phosphate (U/mg)
GAPDH-*T. kodakarensis* KOD1	77.8 ± 7.5	45.1 ± 0.8	49.3 ± 3.0	59.6 ± 1.3	54.6 ± 2.4	52.8 ± 1.0
GAPDH-*M. fervidus*[a]	500	14	–	–	3,500	9
GAPDH-*S. solfataricus*[b]	2,200 ± 500	2.3 ± 1.3	–	–	–	–
GAPDH-*S. pilchardus*[c]	92.0 ± 7.4	37.6 ± 2.9	73.4 ± 8.1	–	–	–

[a, b, c] From previously published paper (Stefan et al. 1988), (Carol et al. 1995), (Baibai et al. 2007)

"–", not shown

only one cysteine, C141. To verify that this cysteine is in the catalytic site of GAPDH-tk, a mutant GAPDH-tk (GAPDH-C141S) was purified, using the same methods as for the wild-type GAPDH-tk (Fig. 4a). Glycolytic activity was measured by detecting NADH production at 80°C, pH 7.0, as shown in "Materials and methods" for both GAPDH-tk and GAPDH-C141S (Fig. 4c). GAPDH-C141S exhibited minimal enzymatic activity, indicating that C141 is an essential active site residue in GAPDH-tk.

Purified GAPDH-C141S was analyzed by gel filtration chromatography and native PAGE (Fig. 4b). Both methods showed that the migration of the mutant is the same as the wild type. These results indicated that disulfide bonds are not required for tetramer formation and that substitution of C141 did not result in major changes in the quaternary structure of GAPDH-tk.

Structure of GAPDH-tk

Based on the gel filtration chromatography results, native GAPDH-tk is a tetramer (~145 kDa) composed of ~37 kDa subunits. To verify the oligomeric structure of GAPDH-tk, we examined the isolated protein by transmission electron microscopy (TEM). Electron micrographs of negatively stained GAPDH-tk show that GAPDH tetramers form globular particles in which the four subunits are symmetrically positioned around the center of the tetramer (Fig. 5a). A total of 487 well-stained particles were translationally aligned and subjected to multivariate statistical analysis. The image averaging revealed a globular-shaped structure, in which the density of the complex was not homogeneous. Two of the subunits appeared equal in density (at 90° and 270°), but the other pair of subunits (at 0° and 180°) were unequal in density (Fig. 5b). This topology may indicate that two of the subunits occupy relative positions that are symmetrical to each other, and, therefore, appear equal in density regardless of the position of the tetramer, while the other pair of subunits is in a non-symmetrical orientation that results in the appearance of unequal densities when many tetramer images are averaged.

Response of GAPDH-tk to oxidative stress

Recent evidence has demonstrated that oxidative stress causes conformational changes in GAPDH (Nakajima et al. 2007; Huang et al. 2009). To understand the response of archaeal GAPDHs to oxidative stress, GAPDH-tk was incubated in the presence or absence of H_2O_2 or nitric oxide (NO) at 80°C for 1 h. Control samples, incubated at 80°C for 1 h in the absence of oxidants, were analyzed by both gel filtration chromatography and native PAGE, and revealed that the molecular mass of GADPH-tk was ~145 kDa (Fig. 6A a, b). This result demonstrated that temperature did not affect the native structure of GAPDH-tk.

In contrast, two peaks were detected by gel filtration chromatography following exposure to H_2O_2 with apparent molecular masses of ~232 kDa (peak 1) and ~145 kDa (peak 2) (Fig. 6Ba). Native PAGE verified the presence of the two high molecular mass complexes, and SDS-PAGE revealed that the complexes consisted of ~37 kDa polypeptides (Fig. 6Bb). In addition, both gel filtration chromatography and native PAGE demonstrated that exposure to NO also caused GAPDH-tk to form much higher molecular mass complexes, ranging in size from ~232 kDa to ~669 kDa (Fig. 6C).

The GAPDH-tk from the above assays was observed by TEM (Fig. 6c). The high molecular mass proteins (~232 kDa, peak 1) from the H_2O_2-treated sample appeared as aggregates (Fig. 6Aa), while the low molecular mass proteins (~145 kDa, peak 2) were similar to the native GAPDH-tk (Fig. 6Ac). In NO-treated GAPDH-tk, the highest molecular mass GAPDH-tk complexes (~669 kDa, peak 1) formed aggregates of short fibrils (Fig. 6Cc) and the high molecular mass GAPDH-tk (~232 kDa, peak 2) formed amorphous agglomerates

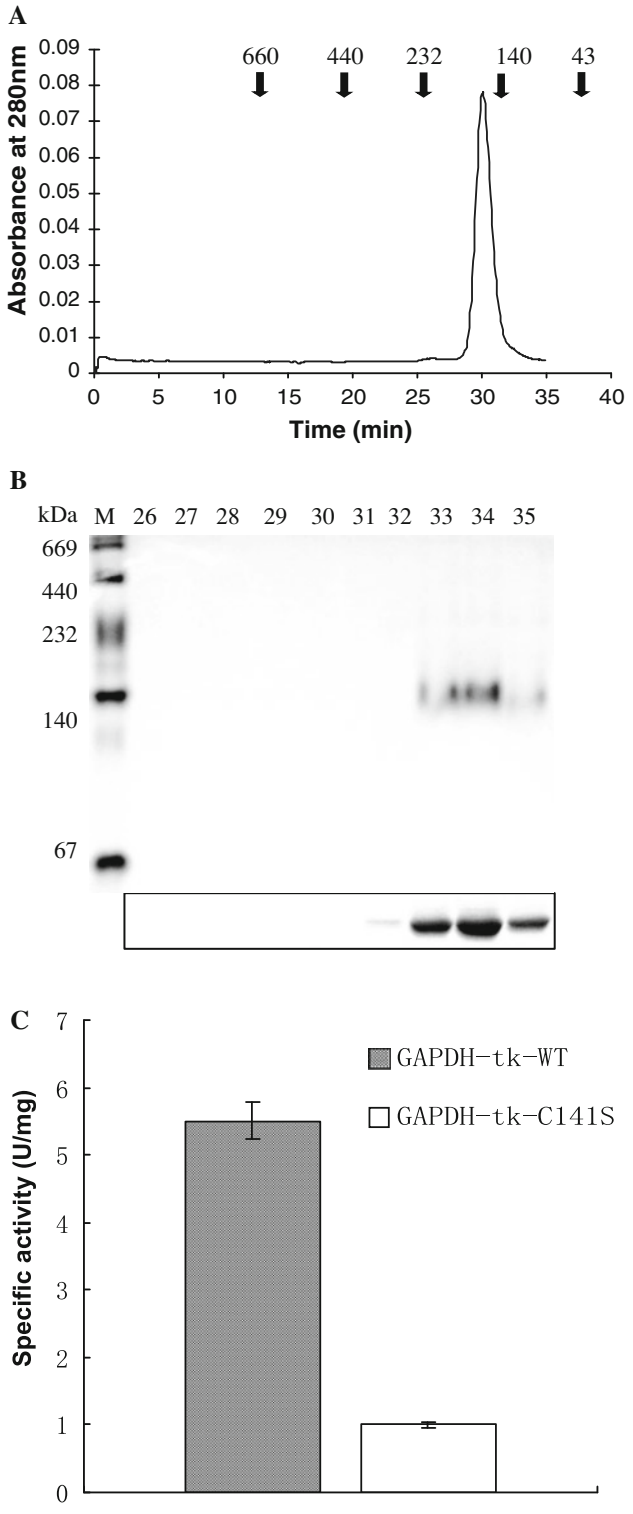

Fig. 4 Comparisons of GAPDH-tk and GAPDH-C141S. **a** Gel filtration chromatography of GAPDH-tk. **b** Gel filtration chromatography fractions were separated by electrophoresis on a 7.5% native gel. The *lower panel* shows the corresponding proteins separated by SDS-PAGE. *Lane M* shows the protein mass standards. **c** Comparison of the glycolytic activity of the GAPDH-tk wild type and the GAPDH mutant (GAPDH-tk-C141S)

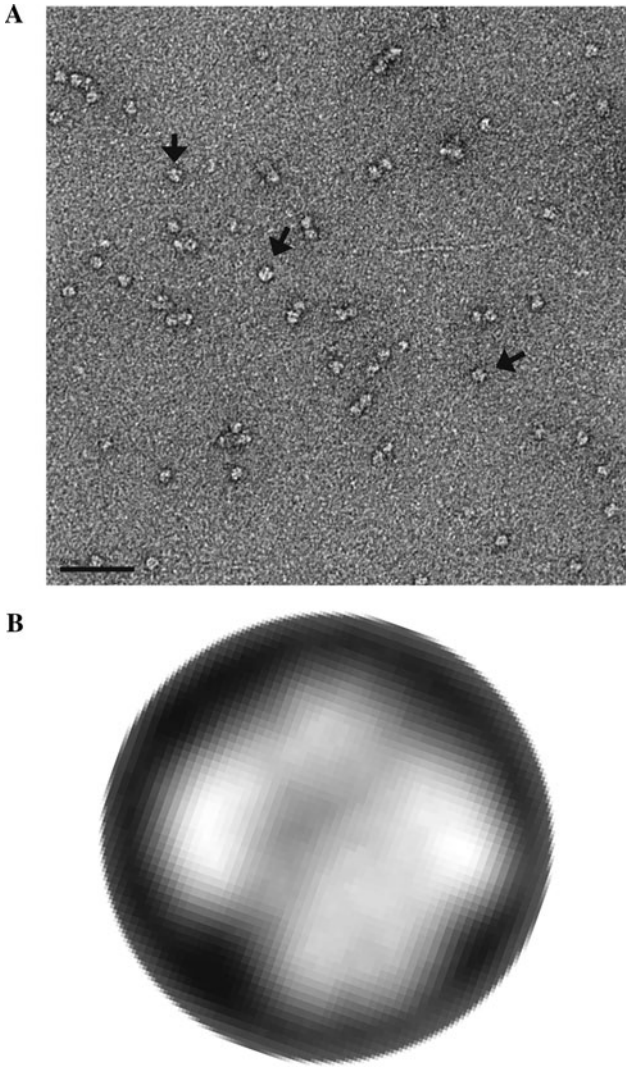

Fig. 5 Electron micrographic and image processing analysis of negatively stained GAPDH-tk. (**a**) Electron micrographs obtained by negative staining of GAPDH-tk with 2% uranyl acetate. The *arrows* indicate GAPDH-tk. **B** The image shows the correlation average of side-on views of GAPDH-tk (averaging of 487 particles)

(Fig. 6Cc), but the low molecular mass GAPDH-tk complex (~145 kDa, peak 3) appeared similar to the native GAPDH-tk (Fig. 6Ac). Furthermore, the aggregates could not be recovered to the native form after the samples were treated by a reducing reagent (DTT) (Fig. S2). Taken together, these results indicate that oxidative stress induces aggregation of GAPDH-tk in vitro.

Discussion

In this study, we reported the catalytic and structural properties of GAPDH-tk and its mutant GAPDH-C141S. In

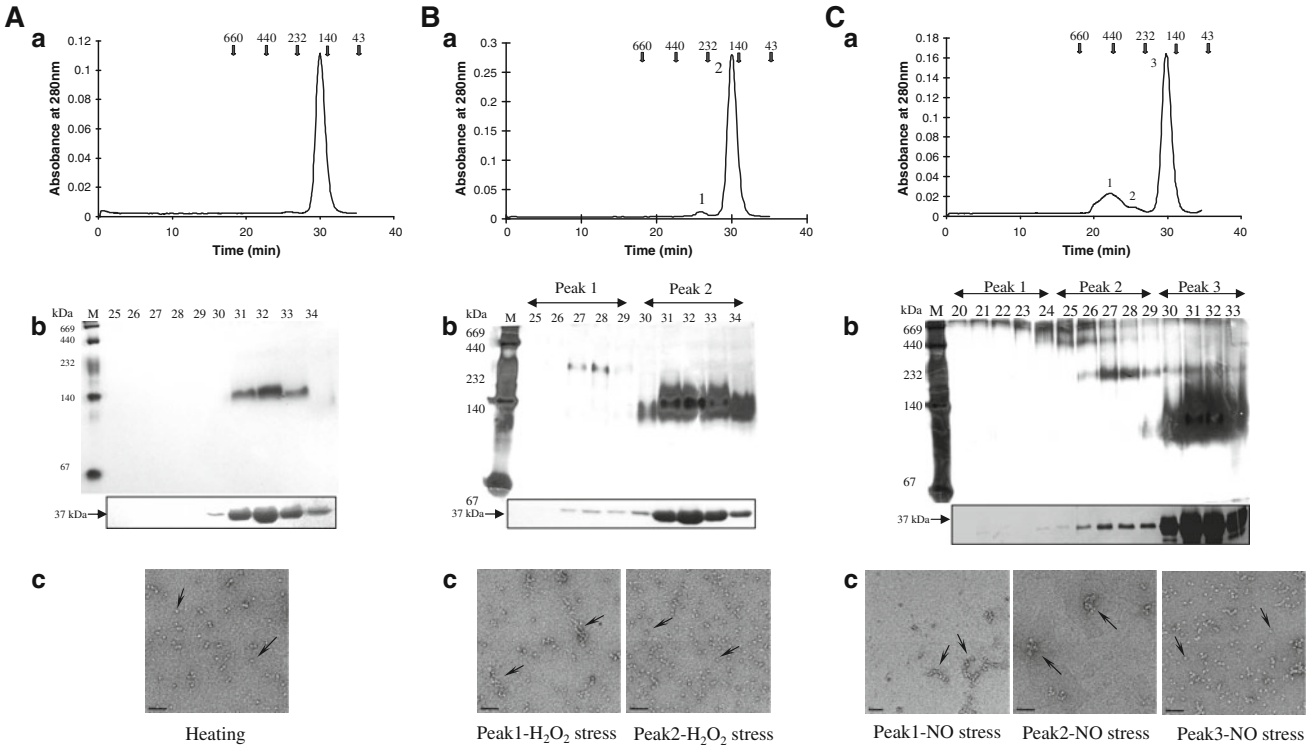

Fig. 6 Effect of H_2O_2 and NO on GAPDH-tk oligomerization. **A** Purified GAPDH-tk was incubated at 80°C for 1 h and loaded onto a Superdex 200 10/300 GL column (**a**). The fractions were analyzed by native PAGE (**b**) and the proteins from the peak fraction were observed by EM (**c**). **B** and **C** Purified GAPDH-tk was treated with H_2O_2 or NO at 80°C for 1 h and separated on a Superdex 200 10/300 GL column (**a**). The fractions were analyzed by native PAGE (**b**) and TEM (**c**)

addition, our results indicate that oxidative stress induces the oligomerization and aggregation of GAPDH-tk.

The K_m for NAD^+ and D-G3P of the *T. kodakarensis* KOD1 GAPDH is lower than the K_m values of the GAPDHs from *M. fervidus* (Stefan et al. 1987), *S. solfataricus* (Carol et al. 1995), and *S. pilchardus* (Baibai et al. 2007) (Table 1). Thus, we proposed that the binding of NAD^+ and D-G3P to GAPDH-tk may be stronger than the substrate–enzyme interactions in the GAPDHs from the other species. The maximal rate of enzymatic activity, V_{max}, is attained when the catalytic sites on the enzyme are saturated with substrate. The V_{max} of GAPDH-tk for NAD^+ is the highest of the enzymes compared in this study and results in the high activity of GAPDH-tk. The half-life of GAPDH-tk is 5 h at 90°C. These results indicate that GADPH-tk is suitable for industrial applications.

Most known GAPDHs are homotetramers. The crystal structure of GAPDH from several organisms has been reported (Isupov et al. 1999; Charron et al. 2000). In *S. solfataricus*, a disulfide bridge crosslinks an α-helix (aa. 138–153) from the catalytic domain to a short α-helix (aa. 120–125) from the nucleotide-binding domain on the surface of the tetramer. Since there is a single cysteine in GAPDH-tk and the GAPDH-tk C141 mutant retained the tetrameric structure, the GAPDH-tk tetrameric structure does not require disulfide bonds. Moreover, the aggregation of GAPDH-tk by oxidative stress should also be independent of disulfide bond formation. This phenomenon is different from oxidant-induced oligomerization and aggregation of GAPDH in the mammalian enzymes, which results from the formation of intermolecular disulfide bonds (Nakajima et al. 2007). The driving force for oligomerization and aggregation of GAPDH-tk may be non-covalent interactions, such as hydrogen bonds and electrostatic interactions (Lucia et al. 2007).

A previous study reported that conformational changes in the structure of GAPDH accompanied increases in the β-sheet content and were critical to the mechanism of oxidative stress-induced aggregation of rabbit GAPDH (Nakajima et al. 2007). GAPDH-tk aggregates were also induced by oxidative stress, although this enzyme possesses only one cysteine, C141, in each monomer. GAPDH-tk aggregates varied in structure. Aggregates of NO-treated GAPDH-tk (~669 kDa) were fibrils, but appeared to be shorter than fibrillar aggregates of rabbit GAPDH. Additionally, amorphous agglomerates of NO-treated GAPDH-tk (~232 kDa) were observed. Thus, oxidative stress may alter the normal conformation of GAPDH-tk.

Our study is the first reported description of aggregates of an archaeal GAPDH under oxidative stress. The mechanisms of oxidative stress-induced aggregation of GAPDH-tk will require further examination in future work.

References

Atomi H, Fukui T, Kanai T, Morikawa M, Imanaka T (2004) Description of *Thermococcus kodakaraensis* sp. nov., a well studied hyperthermophilic archaeon previously reported as *Pyrococcus* sp. KOD1. Archaea 1:263–267

Baibai T, Oukhattar L, Moutaouakkil A, Soukri A (2007) Purification and characterization of glyceraldehyde-3-phosphate dehydrogenase from European pilchard *Sardina pilchardus*. Acta Biochim Biophys Sin 39:947–954

Brunner N, Brinkmann H, Siebers B, Hensel R (1998) NAD^+-dependent glyceraldehyde-3-phosphate dehydrogenase from *Thermoproteus tenax*. J Biol Chem 273:6149–6156

Brunner N, Siebers B, Hensel R (2001) Role of two different glyceraldehyde-3-phosphate dehydrogenases in controlling the reversible Embden–Meyerhof–Parnas pathway in *Thermoproteus tenax*: regulation on protein and transcript level. Extremophiles 5:101–109

Carol EJ, Toni MF, Don AC, Jennifer AL, Peter WP (1995) The phosphoglycerate kinase and glyceraldehyde-3-phosphate dehydrogenase genes from the thermophilic archaeon *Sulfolobus solfataricus* overlap by 8-bp. Isolation, sequencing of the genes and expression in *Escherichia coli*. Eur J Bio Chem 233:800–808

Charron C, Talfournier F, Isupov MN, Littlechild JA, Branlant G, Vitoux B, Aubry A (2000) The crystal structure of D-glyceraldehyde-3-phosphate dehydrogenase from the hyperthermophilic archaeon *Methanothermus fervidus* in the presence of $NADP^+$ at 2.1 Å resolution. J Mol Biol 29:481–500

Cleland WW (1963) The kinetics of enzyme-catalyzed reactions with two or more substrates or products: II. Inhibition: nomenclature and theory. Biochim Biophys Acta 67:173–187

Elkina Y, Kuravsky ML, El'darov MA, Stogov SV, Muronetz VI, Schmalhausen EV (2010) Recombinant human sperm-specific glyceraldehyde-3-phosphate dehydrogenase: structural basis for enhanced stability. Biochim Biophys Acta 1804:2207–2212

Engel M, Seifert M, Theisinger B, Seyfert U, Welter C (1998) Glyceraldehyde-3-phosphate dehydrogenase and Nm23–H1/nucleoside diphosphate kinase A. J Biol Chem 273:20058–20065

Fabry S, Reinhar Hensel (1987) Purification and characterization of D-glyceraldehyde-3-phosphate dehydrogenase from the thermophilic archaebacterium *Methanothermus fervidus*. Eur J Bio Chem 165:147–155

Fourrat L, Iddar A, Soukri (2007) Purification and characterization of cytosolic glyceraldehyde-3-phosphate dehydrogenase from the dromedary camel. Acta Biochim Biophys Sin 39:148–154

Hara M, Snyder S (2006) Nitric oxide–GAPDH–Siah: a novel cell death cascade. Cell Mol Neurobiol 26:525–536

Hara MR, Agrawal N, Kim SF, Cascio MB, Fujimuro M, Ozeki Y, Takahashi M, Cheah JH, Tankou SK, Hester LD, Ferris CD, Hayward SD, Snyder SH, Sawa A (2005) S-nitrosylated GAPDH initiates apoptotic cell death by nuclear translocation following Siah1 binding. Nat Cell Biol 7:665–674

Hegerl R (1996) The EM program package: a platform for image processing in biological electron microscopy. J Struct Biol 116:30–34

Huang J, Hao L, Xiong N, Cao X, Liang Z, Sun S, Wang T (2009) Involvement of glyceraldehyde-3-phosphate dehydrogenase in rotenone-induced cell apoptosis: relevance to protein misfolding and aggregation. Brain Res 1279:1–8

Isupov MN, Fleming TM, Dalby AR, Crowhurst GS, Bourne PC, Littlechild JA (1999) Crystal structure of the glyceraldehyde-3-phosphate dehydrogenase from the hyperthermophilic archaeon *Sulfolobus solfataricus*. J Mol Biol 291:651–660

Kim KI, Cheong GW, Park SC, Ha JS, Woo KM, Choi SJ, Chung CH (2000) Heptameric ring structure of the heat-shock protein ClpB, a protein-activated ATPase in *Escherichia coli*. J Mol Biol 303:655–666

Launay JF, Jellali A, Vanier MT (1989) Glyceraldehyde-3-phosphate dehydrogenase is a microtubule binding protein in a human colon tumor cell line. Biochim Biophys Acta 996:103–109

Littlechild JA, Isupov M (2001) Glyceraldehyde-3-phosphate dehydrogenase from *Sulfolobus solfataricus*. Methods Enzymol 331:105–117

Lorentzen E, Hensel R, Knura T, Ahmed H, Pohl E et al (2004) Structural basis of allosteric regulation and substrate specificity of the non-phosphorylating glyceraldehyde 3-phosphate dehydrogenase from *Thermoproteus tenax*. J Mol Biol 341:815–828

Lucia B, Ivano B, Armando D, Stefania G, Edith BG, Manuele M, Joan SV, Miguela V, Julian PW (2007) Metal-free superoxide dismutase forms soluble oligomers under physiological conditions: a possible general mechanism for familial ALS. Proc Natl Acad Sci USA 104:11263–11267

Marco S, Ureña D, Carrascosa JL, Waldmann T, Peters Jr, Hegerl R, Pfeifer Gn, Sack-Kongehl H, Baumeister W (1994) The molecular chaperone TF55: Assesment of symmetry. FEBS Lett 341:152–155

Nakajima H, Amano W, Fujita A, Fukuhara A, Azuma YT, Hata F, Inui T, Takeuchi T (2007) The active site cysteine of the proapoptotic protein glyceraldehyde-3-phosphate dehydrogenase is essential in oxidative stress-induced aggregation and cell death. J Biol Chem 282:26562–26574

Park SC, Jia B, Yang JK, Le Van D, Shao YG, Han SW, Jeon YJ, Chung CH, Cheong GW (2006) Oligomeric structure of the ATP-dependent protease La (Lon) of *Escherichia coli*. Mol Cells 21:129–134

Roitel O, Sergienko E, Branlant G (1999) Dimers generated from tetrameric phosphorylating glyceraldehyde-3-phosphate dehydrogenase from *Bacillus stearothermophilus* are inactive but exhibit cooperativity in NAD binding. Biochemistry 38:16084–6091

Russo AD, Rullo R, Masullo M, Ianniciello G, Arcari P, Bocchini V (1995) Glyceraldehyde-3-phosphate dehydrogenase in the hyperthermophilic archaeon *Sulfolobus solfataricus*: characterization and significance in glucose metabolism. Biochem Mol Biol Int 36:123–135

Sand O, Petersen IM, Jørgen J, Iversen L (1994) Purification and some properties of glyceraldehyde 3-phosphate dehydrogenase from *Synechococcus* sp. Antonie Van Leeuwenhoek 65:133–142

Saxton WO, Pitt TJ, Horner M (1979) Digital image processing: the Semper system. Ultramicroscopy 4:343–353

Sirover MA (1996) Emerging new functions of the glycolytic protein, glyceraldehyde-3-phosphate dehydrogenase, in mammalian cells. Life Sci 58:2271–2277

Stefan F, Anselm L, Wolfram B, Reinhard H (1988) Expression of the glyceraldehyde-3-phosphate dehydrogenase gene from the extremely thermophilic archaebacterium *Methanothermus fervidus* in *E. coli*. FEBS Lett 237:213–217

Tisdale EJ (2001) Glyceraldehyde-3-phosphate dehydrogenase is required for vesicular transport in the early secretory pathway. J Biol Chem 276:2480–2486

Tristan C, Shahani N, Sedlak TW, Sawa A (2011) The diverse functions of GAPDH: views from different subcellular compartments. Cell Signal 23:317–323

Van Heel M, Frank J (1981) Use of multivariate statistics in analysing the images of biological macromolecules. Ultramicroscopy 6:187–194

Wrba A, Schweiger A, Schultes V, Jaenicke R, Závodszky P (1990) Extremely thermostable D-glyceraldehyde-3-phosphate dehydrogenase from the eubacterium *Thermotoga maritima*. Biochemistry 29:7584–7592

Yun M, Park CG, Kim JY, Park HW (2000) Structural analysis of glyceraldehyde 3-phosphate dehydrogenase from *Escherichia coli*: direct evidence of substrate binding and cofactor-induced conformational changes. Biochemistry 39:10702–10710

Zwick P, Fabry S, Bogedain C, Haas A, Hensel R et al (1990) Glyceraldehyde-3-phosphate dehydrogenase from the hyperthermophilic archaebacterium *Pyrococcus woesei*: characterization of the enzyme, cloning and sequencing of the gene, and expression in *Escherichia coli*. J Bacteriol 172:4329–4338